第 16 卷　第 6 期
2008 年 12 月

含　能　材　料
CHINESE JOURNAL OF ENERGETIC MATERIALS

Vol. 16, No. 6
December, 2008

文章编号： 1006-9941(2008)06-0745-08

Photocatalytic Degradation of HMX and RDX Wastewater with CdS/Cu Nanophotocatalyst

Hamid Reza Pouretedal, Mohammad Hossien Keshavarz, Mohammad Hasan Yosefi, Arash Shokrollahi, Abbas Zali

(*Faculty of Science, Malek-ashtsr University of Technology, Shahin-shahr, Iran*)

Abstract: The wastewater with HMX and RDX was treated by photodegradation process in the presence of cadmium sulfide doped with copper as photocatalyst under UV and Vis irradiations. The influence on the degration of Cu% as dopant in CdS/Cu nanoparticles, pH of solution, dosage of photocatalyst and concentration of explosives were studied. The XRD patterns and UV-Vis spectra were used to characterize the nanoparticle. Results show that the degradation efficiency for HMX and RDX wastewater reaches 85% -88% in the presence of $Cd_{0.95}Cu_{0.05}S$ under 180 min UV irradiation. The dosage of 160.0 mg · L^{-1} of photocatalyst and the pH of 7 are the optimum. A gradual decrease in degradation at the first two cycles is seen.

Key words: cadmium sulfide; nanoparticle; photodegradation; photocatalyst; RDX; HMX

CLC number: TJ55; O63　　**Document code**: A

1 Introduction

Among various physical, chemical and biological techniques for treatment of wastewaters, heterogeneous photocatalysis has been considered as a cost-effective alternative for water remediation[1-3]. Photocatalysis is a process by which a semiconducting material absorbs light of energy more than or equal to its band gap, thereby generating holes and electrons, which can further generate free-radicals in the system to oxidize the substrate. The free-radicals are very efficient oxidizers of organic matter. Nano-scale semiconductor particles possess higher surface area-to-volume ratio than their bulk counterparts, and thus allow for greater photon absorption on the photocatalyst surface. Moreover, recombination of the electron-hole pair within the semiconductor particle is drastically reduced as particle size decreases. With decreasing the particle size of semiconductor to nanometer-size scale, the band-gap energy increased greatly, which in turn led to higher redox potentials in the system. Therefore, the nano-scale semiconductor is expected to have higher photocatalytic activity than its bulk[4-6].

One of the attractive research fields in recent years is synthesis of various sizes and shapes of semiconductor materials nanoparticles. The goal of these activities is improving the performance and utilization of nanoparticles in various applications from sensing devices to photonic materials in molecular electronics and to advanced oxidation techniques (AOTs). The size and shape dependent optical and electronic properties of these nanoparticles make an interesting case for exploiting them in light induced chemical reactions. Of particular emphasis in this review is their application in advanced oxidation processes. In this context, nanoparticles are commonly employed as photocatalysts[5-6]. Nanoparticles of cadmium sulfide as a semiconductor were prepared by several methods[7-10]. Agostiano and co-works was synthesized nanoparticles of CdS in a quaternary "water-in-oil" microemulsion formed by a cationic surfactant cetyltrimethylammonium bromide (CTAB), pentanol, *n*-hexane and water[11]. Nanoparticles of CdS with diameter of 3.0 nm were prepared by the sonochemical reduction of a mixed of $CdCl_2$, $Na_2S_2O_3$ and isopropyl alcohol by Wang and co-workers[12].

High explosives are widely used in the field of national defense and industrial engineering owing to the high chemical energy released on explosion, and therefore a great deal of monition waste is produced[13]. Among the various explosives, hexahydro-1,3,5-trinitro-1,3,5-triazine (RDX) and octahydro-1,3,5,7-tetranitro-1,3,5,7-tetrazocine (HMX) are two main explosive substances used by monition industries. However, these substances are carcinogenic[14-18] and , therefore , the corresponding

---

Received Date: 2008-03-18; **Revised Date**: 2008-06-19

Corresponding author: e-mail: HR_POURETEDAL@ mut-es. ac. ir

wastes present both environmental and health concerns[19-20]. Additionally, these substances are normally difficult to degrade. Therefore, the soils and groundwater near the munitions factories are seriously contaminated[21].

This article reports the application of nanoparticles of cadmium sulfide doped with Cu as photocatalyst in degradation of RDX and HMX in wastewater as two pollutants under ultraviolet (UV) and visible (Vis) irradiations. The effective parameters on the degradation efficiency such as % Cu in CdS/Cu nanoparticles, pH of solution and dosage of photocatalyst were optimized for achievement the maximum efficiency. Also, the influence of UV and Vis irradiations was compared with each other as two sources of irradiation.

2 Experimental

2.1 Materials

$CdCl_2$ and $CuCl_2 \cdot 2H_2O$, all from Merck, as source of Cd^{2+} and Cu^{2+} ions were used and sodium sulfide with nine water molecules ($Na_2S \cdot 9H_2O$, Merck) was used as source of sulfide ion. 2-Mercaptoethanol (2-hydroxyethanthiol, $HOCH_2CH_2SH$) as capping agent and isopropyl alcohol as solvent were prepared from Merck Company and used as received. Hydrochloric acid and sodium hydroxide were applied for variation of pH of sample solutions. Methanol and acetonitrile with chromatographic grade were prepared from Merck Company. Double-distilled water was used for preparation of solutions and tap-water (Ca^{2+}; 3.5 $mg \cdot L^{-1}$, Mg^{2+}; 2.2 $mg \cdot L^{-1}$ and Na^{+}; 2.5 $mg \cdot L^{-1}$) was used for preparation of the simulated HMX and RDX wastewater.

The explosives of HMX and RDX (Fig. 1) with highest purity were synthesized by the defense research group of Malek-ashtar University of Technology. The purity of explosives (greater than 99%) was confirmed by high-performance liquid chromatography (HPLC). The simulated HMX and RDX wastewaters were prepared by dissolving of 4.0 and 40.0 mg, respectively, in 10 mL of acetone and the solution was then added slowly to a 1000 mL beaker containing 800 mL of water (80 ℃)[14]. The beaker was heated up continuously until no acetone could be detected and the process lasted for ca. 4 h. After cooled at room temperature, the solution was transferred to a brown capacity bottle of 1000 mL, and diluted with water to the graduation mark. The prepared solutions with concentration of 4.0 and 40.0 $mg \cdot L^{-1}$ were the simulated HMX and RDX, respectively, wastewaters and stored at room temperature for later use.

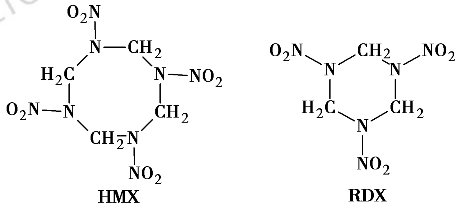

Fig. 1 Structure of HMX and RDX

2.2 Catalyst preparation

The controlled precipitation and co-precipitation methods were used for preparation of $Cd_{1-X}S/Cu_X$ ($X = 0$, 0.02, 0.05 and 0.10) nanoparticles. To 50 mL homogeneous solution of 0.01 M $CdCl_2$ and $CuCl_2$ with mole ratio $[Cu^{2+}]/[Cd^{2+}] = X$ in a balloon (three-vent), 50 mL solution of 0.1 M mercaptoethanol were added, gradually, whereas the solution was stirred on a magnetic stirrer. Then, 50 mL solution of 0.01 M sodium sulfide was added drop by drop using a decanter vessel (each 6 - 8 s, one drop) under nitrogen atmosphere while the mixture was stirred vigorously at room temperature. The prepared nanoparticles of $Cd_{1-X}Cu_XS$ were deposited at the end of process. In order to separation of resulting precipitate, the mixture was centrifuged at 4000 rpm and the nanoparticles of $Cd_{1-X}Cu_XS$ were washed three times with water for eliminations of unreacted ions. Finally, it was washed three times with isopropyl alcohol. The cleaned powders were dried for about 10 h at 80 ℃ until complete evaporation of the solvent was achieved. To this way, the nanoparticles of CdS and CdS/Cu with percentages of 2%, 5% and 10% of doped ion were purchased.

2.3 Apparatus

Chromatographic system of Agilent Technologies (HP) consisting of a quaternary pump with micro vacuum degasser, a 20 μL injector (Agilent 1200 series manual injector), a 1200 series ultraviolet variable wavelength detector and a temperature controlling module for HPLC-UV analysis was used. Typically, 2 and 20 μL of the RDX and HMX, respectively, containing wastewater were directly injected into a Microsorb-MV 100 C18 column (25 cm × 4.6 mm, 5 μm). The mobile phase of the column was a mixture of methanol and water with volume ratio of 50 : 50 and the flow-rate was 1 mL · min^{-1}. The column temperature was maintained at 30 ℃ and the running time was 20 min. An ultraviolet detector set at 254 nm was used. The analyzing of chromatograms was done using HPLC 2D chemstation software.

A Siemens D-5005 diffractometer using CuK$_\alpha$ irradiation ($\lambda = 1.5418$ Å) was used for X-ray powder diffraction (XRD) patterns of nanoparticles. Transmission electron micrographs (TEMs) of the nanoparticles were taken by a JEOL JEM-1200EXII electron microscope operating at 120 kV. The supporting grids were formvar-covered, carbon-coated, 200-mesh copper grids. The UV-Vis absorption spectra of 10 mM solutions of nanoparticles were recorded by using an UV-Vis spectrophotometer Perkin-Elmer Lambda 2 at room temperature. The sol transparent samples of nanoparticles were prepared with dispersing of them in isopropyl alcohol. The pH value of the solutions was determined by a Metrohm 661 pH meter.

2.4 Photodegradation experiments

A photocatalytic reactor system was used for photodegradation experiments. This bench-scale system consisted of a cylindrical Pyrex-glass cell with 1.0 L capacity, 10 cm inside diameter and 15 cm height. The lamps of 100 W mercury and 500-W halogen as UV and Vis light sources, respectively, were placed in a 5 cm diameter quartz and/or glass tube with one end tightly sealed by a Teflon stopper. For assurance from source of visible light, a cutoff filter was applied to remove wavelengths below 420 nm. The lamp and the tube were then immersed in the photoreactor cell with a light path of 3.0 cm. The photoreactor was filled with 0.5 L of 4.0 and 40.0 mg · L^{-1} of HMX and RDX, respectively, as pollutant and 40.0 – 200.0 mg · L^{-1} of nanoparticles as nanophotocatalyst. The whole reactor was cooled with a water-cooled jacket on its outside and the temperature was kept at 25 ℃. A magnetic stirrer was used for stirring of solutions in order to ensure that the suspension of the catalyst was uniform during the course of the reaction. The samples were collected at regular intervals, filtered through Millipore membrane filters, and centrifuged to remove the nanocatalyst particles that exist as undissolved particles in the samples. The resulting samples were used for determination degradation efficiency of explosives.

The peak area of RDX and/or HMX in HPLC chromatograms before and after degradation in the selected time intervals was used for determination of degradation efficiency ($D\%$). The degradation efficiency was calculated as:

$$D\% = 100 \times [(S_o - S)/S_o]$$

where S_o and S are the peak areas of explosive before and after degradation in selected time intervals, respectively.

The effective parameters on yield of process such as pH, concentration of explosives and amount of photocatalyst were studied in irradiation time of 180 min of UV and Vis lights. The degradation of nitramine explosives was investigated in the presence of nanoparticles of CdS and CdS/Cu with percentages of 2%, 5% and 10% of doped ion as photocatalyst at room temperature.

3 Results and discussion

3.1 Characterization of nanoparticles

The characterization of nanoparticles includes CdS and CdS/Cu (2%, 5% and 10%) was determined by XRD patterns and UV-Vis spectra. The XRD patterns of CdS doped with 5% Cu as is shown in Fig. 2. Three broad peaks with 2θ vales 26.5°, 44.0° and 52.0° corresponding to the (111), (220) and (311) plans of CdS, respectively, therefore the powder is pure cubic CdS phase. Due to the size effect, the XRD peaks are broadened as the particles become smaller. The diameter of CdS nanoparticles estimated from Scherrer formula is smaller than 5.0 nm[22-23]. Also, transmission electron micrographs (TEM) images confirmed the formation of CdS/Cu(5%) nanoparticles with diameters of (6.0 ± 1.0) nm (Fig. 3).

In Fig. 4, the absorption spectra of CdS and CdS/Cu(5%) nanoparticles in isopropyl alcohol solvent are shown. The UV absorption analysis of the sample provides the information relating to the size of particles. The absorption shoulder of nanoparticles are seen about 370 – 380 nm, while, the absorption shoulder for macrocrystalline CdS is seen at about 510 nm with band-gap energy of 2.4 eV. Therefore, this blue shift and correlation between band edge and quantum dot size indicates that the size of prepared particles is less than 10.0 nm[24-25].

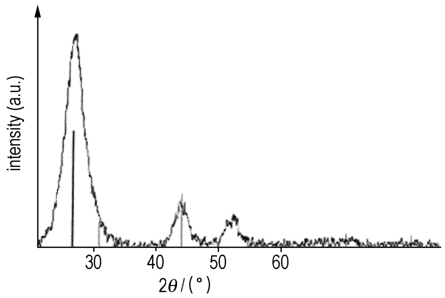

Fig. 2 X-ray diffraction pattern of CdS/Cu(5%) nanocrystals

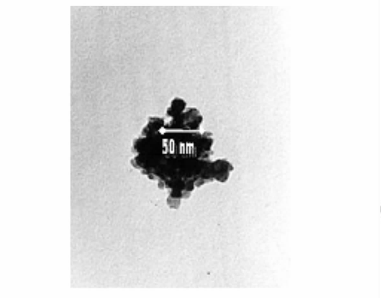

Fig. 3 TEM image of nanoparticles of CdS/Cu(5%)

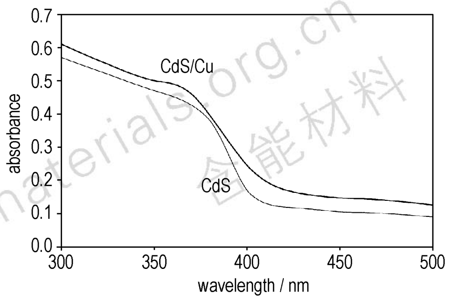

Fig. 4 UV-Vis spectra of nanocrystals of CdS and CdS/Cu(5%) in isopropyl solution

3.2 Photodegradation of HMX and RDX using nanophotocatalysts

Photodegradation of HMX and RDX explosives with initial concentration of 4.0 and 40.0 mg · L^{-1}, respectively, and after irradiation time of 180 min under UV light are shown in Fig. 5. The experiments were done in the absence and in the presence of macrocrystalline and nanocrystalline of CdS with dosage 120.0 mg · L^{-1}. The efficiency of photodegradation is obtained as: without photocatalyst < macroparticles of CdS < nanoparticles of CdS, for HMX and RDX explosives. In process of photodegradation of organic pollutants in the presence of photocatalysts such as cadmium sulfide, the electron/hole pair is obtained from photoexcitation of CdS using an irradiation with suitable energy[24]. With transfer electrons from valance band of semiconductor to conductance band, the active fundamental particles of holes and electrons are formed in valance and conductance bands, respectively. The holes with high oxidative potential leads to direct and indirect oxidation of explosives. The hydroxide reactive radicals (OH^-) were formed from combination of holes with water molecules and/or hydroxide anions and lead to indirect oxidation explosives. The radical hydroxide with $E^{\circ} = +3.06$ V is a strong oxidative and oxidize explosives as non-selective to mineral species as partial or complete[26-27].

$$\mathrm{CdS/Cu} + h\nu \longrightarrow h^+_{\mathrm{VB}} + e^-_{\mathrm{CB}} \tag{1}$$

$$h^+_{\mathrm{VB}} + \mathrm{H_2O} \longrightarrow {}^{\cdot}\mathrm{OH} + \mathrm{H^+} \tag{2}$$

$$h^+_{\mathrm{VB}} + \mathrm{OH^-} \xrightarrow{-} {}^{\cdot}\mathrm{OH} \tag{3}$$

The total number of free carriers (electrons/holes) on the surface of photocatalyst determines the efficiency of catalyst. The volume recombination of electrons and holes dominates in large particles. This condition largely reduces the number of free charges on the surface and deteriorates the photocatalytic activity. For nanoparticles, the transportation length of electron/hole from crystal interface to the surface is short, which helps to accelerate the migration rate of electron/hole to the surface of the nanoparticle to participate the reaction process[28]. The increasing of the lifetime of free charges (electrons/holes) as well as increasing of accessible surface of photocatalysts in nanoparticles[29] leads to increasing of photodegradation efficiency of explosives.

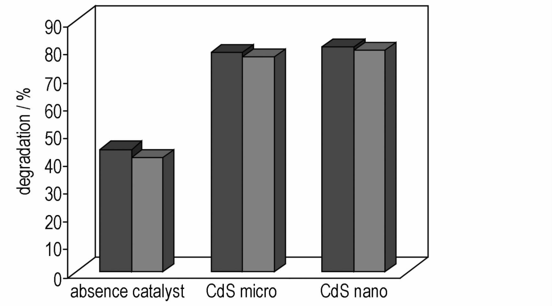

Fig. 5 Photodegradation of HMX (4.0 mg · L^{-1}, black color) and RDX (40.0 mg · L^{-1}, gray color) in the absence, macrocrystalline and nanocrystalline of CdS with dosage 120.0 mg · L^{-1} after irradiation time of 180 min

As mentioned, the number and the lifetime of free carriers (electrons/holes) are particle size- and dopant-dependent. The effect of dopant percent on the photodegradation efficiency of explosives were studied in the presence of cadmium sulfide doped with different percents of copper (2%, 5% and 10%). The nanophotocatalysts with dosage of 120.0 mg · L^{-1} were applied in irradiation time of 180 min. The obtained results are given in Fig. 6. On the other hand, the most degradation for both explosives was occurred using $Cd_{0.95}Cu_{0.05}S$ as photocatalyst in among of prepared nanoparticles. Doping of CdS with other transition metal ions offers a way to trap charge carriers and extend the lifetime of one or both of the charge carriers. Consequently, dopants enhance the efficiency of the photocatalyst[30-32].

The Cu^{2+} ion with $E^{o} = +0.337$ V acts an oxidizing agent. In other word, the Cu^{2+} ion is reduced to Cu^{+} ion by a hole produced in semiconductor. The resulting ion (Cu^{+}) is a strong oxidative ($E^{o} = +0.521$ V) and hence it is also an oxidizing agent for organic pollutants. As a result, in these conditions, in beside of holes and hydroxyl radicals, Cu^{2+} and Cu^{+} ions, also, act as oxidizing agents and the rate of degradation increases.

3.3 Photocatalytic degradation kinetics

The results of photocatalytic degradation kinetics indicated that the destruction rates of photocatalytic oxidation of various organic pollutants over illuminated heterogeneous photocatalysts such as TiO_2 fitted the Langmuir-Hinshelwood (L-H) kinetics model[33-34]:

$$r = -\mathrm{d}C/\mathrm{d}t = kKC/(1 + KC)$$

where r is the oxidation rate of the reactant ($\mathrm{mg \cdot L^{-1} \cdot min^{-1}}$), C is the concentration of the reactant ($\mathrm{mg \cdot L^{-1}}$), t the illumination time, k the reaction rate constant ($\mathrm{mg \cdot L^{-1} \cdot min^{-1}}$), and K is the adsorption coefficient of the reactant ($\mathrm{L \cdot mg^{-}}$). When the chemical concentration C_o is small the above equation can be simplified to an apparent first-order equation:

$$\ln(C_o/C) = kt$$

A plot of $\ln(C_o/C)$ versus time represents a straight line, the slope of which upon linear regression equals the apparent first-order rate constant k. Generally, first-order kinetics is appropriate for the entire concentration range up to few ppm and several studies were reasonably well fitted by this kinetic model. It has been agreed that the expression for the rate of photomineralization of organic substrates such as dyes with irradiated TiO_2 follows the Langmuir-Hinshelwood (L-H) law. The calculated results indicate that the first-order model gives a better fit. The apparent degradation rate constant (k) of explosives with initial concentrations of 4.0 and 40.0 $\mathrm{mg \cdot L^{-1}}$ of HMX and RDX, respectively, were calculated and collected in Table 1.

3.4 Optimization of photocatalytic conditions

Figure 7 illustrates photodegradation of HMX and RDX in the different dosage (40.0 - 200.0 $\mathrm{mg \cdot L^{-1}}$) of nanocatalysts $Cd_{0.95}Cu_{0.05}S$ with irradiation time of 180 min. The initial rate of photocatalytic degradation of many pollutants is a function of the photocatalyst dosage[35-36]. It is evident that the degradation rates of HMX and RDX does not increase linearly with increasing of nanocatalyst content. Indeed, maximum value achieves at a medium loading of 160 $\mathrm{mg \cdot L^{-1}}$ which is due to two competitive processes. In general, the greater the amount of catalyst, the higher the reaction rates should be, due to the fact that more holes and hydroxyl radicals are generated. However, more $Cd_{0.95}Cu_{0.05}S$ also induces greater aggregation of the $Cd_{0.95}Cu_{0.05}S$ particles, with the effect that the $Cd_{0.95}Cu_{0.05S}$ particle size increases and the specific surface area of $Cd_{0.95}Cu_{0.05}S$ decreases, leading to a reduction in reaction rate.

Table 1 Apparent degradation rate constant (k) and standard deviation ($n = 3$) of HMX and RDX with initial concentrations of 4.0 and 40.0 $\mathrm{mg \cdot L^{-1}}$, respectively

photocatalyst	HMX	RDX
without photocatalyst	$(3.2 \pm 0.3) \times 10^{-3}\ \mathrm{min^{-1}}$	$(2.9 \pm 0.2) \times 10^{-3}\ \mathrm{min^{-1}}$
CdS macrocrystaline	$(8.6 \pm 0.2) \times 10^{-3}\ \mathrm{min^{-1}}$	$(8.2 \pm 0.3) \times 10^{-3}\ \mathrm{min^{-1}}$
CdS nanocrystaline	$(9.1 \pm 0.2) \times 10^{-3}\ \mathrm{min^{-1}}$	$(8.8 \pm 0.3) \times 10^{-3}\ \mathrm{min^{-1}}$
$Cd_{0.98}Cu_{0.02}S$	$(9.6 \pm 0.4) \times 10^{-3}\ \mathrm{min^{-1}}$	$(9.3 \pm 0.4) \times 10^{-3}\ \mathrm{min^{-1}}$
$Cd_{0.95}Cu_{0.05}S$	$(9.9 \pm 0.3) \times 10^{-3}\ \mathrm{min^{-1}}$	$(9.7 \pm 0.4) \times 10^{-3}\ \mathrm{min^{-1}}$
$Cd_{0.90}Cu_{0.10}S$	$(9.8 \pm 0.3) \times 10^{-3}\ \mathrm{min^{-1}}$	$(9.7 \pm 0.4) \times 10^{-3}\ \mathrm{min^{-1}}$

It is well known that pH influences the rate of photocatalytic degradation of some organic compounds. It is also an important operational variable in practical wastewater. Degradation of HMX and RDX, 4.0 and 40.0 $\mathrm{mg \cdot L^{-1}}$, respectively, was studied in amplitude pH of 2.0 - 12.0 in the presence of nanocatalyst $Cd_{0.95}Cu_{0.05}S$ (160.0 $\mathrm{mg \cdot L^{-1}}$). The results for irradiation time of 180 min are shown in Fig. 8. The maximum degradation efficiency was obtained in neutral pH 7 for both explosives. In the presence of $Cd_{0.95}Cu_{0.05}S$ and in pH 7, degradation efficiency is obtained with 91.0% and 93.0% RDX and HMX, respectively.

The parameters that vary with respect to change in pH are concentration of OH radicals, surface charge on the catalyst, ionization state of the substrate, etc. The higher degradation rate at higher pH is attributed to the higher concentration of OH radicals at higher pH. A low pH is associated with a positively charged surface which cannot provide hydroxyl group which are needed for hydroxyl radical formation[37-38]. In pH 7, because neutrality charge surface of catalyst, the most adsorption of molecules of RDX and/or HMX was occurred and the maximum degradation were obtained. But, the degradation of explosives was inhibited when the pH value was more than 7 because the hydroxyl ions would compete with explosives molecules in adsorption on the surface of photocatalysts.

As seen from Fig. 9, the rate of degradation and therefore the degradation efficiency increases with increasing of HMX and RDX concentrations. Also, in the lower concentrations of explosives, degradation efficiency increases and reaches 85% -88% with passing of time. Therefore, the final degradation efficiency is independent of the initial concentrations of HMX and RDX in the wastewater samples[14].

3.5 Reproducibility of the nanocatalyst CdS/Cu(5%)

Figure 10 reports the reproducibility of $Cd_{0.95}Cu_{0.05}S$ as nanocatalysts for photodegradtion of explosives during a three cycles experiment. Each experiment was carried out under identical conditions of 4.0 and 40.0 mg · L^{-1} of HMX and RDX, respectively, 160.0 mg · L^{-1} of nanocatalyst, pH of 7, irradiation time of 180 min and at room temperature. The concentration of explosives was adjusted back to its initial values after each degradation experiment. A gradual decrease in the photoactivity of nanocatalysts was observed at the first two cycles in Fig. 10. But, decreasing of the degradation efficiency was observed intense after the first and second cycles.

3.6 Photodegradation of HMX and RDX under visible irradiation

The degradation of HMX and RDX under Vis irradiation was studied at optimized conditions of photodegradation with UV light. In Fig. 11, degradation efficiency in time duration of 1 8 0 min are shown and compared with

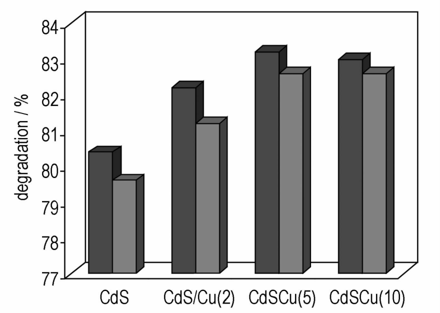

Fig. 6 Photodegradation of HMX (4.0 mg · L^{-1}, black color) and RDX (40.0 mg · L^{-1}, gray color) in the presence of CdS and CdS/Cu nanocatalysts with dosage 120.0 mg · L^{-1} after irradiation time of 180 min

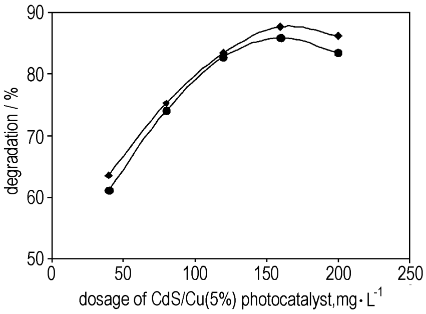

Fig. 7 Photodegradation of HMX (◆, 4.0 mg · L^{-1}) and RDX (●, 40.0 mg · L^{-1}) in different dosage of CdS/Cu(5%) nanocatalysts after irradiation time of 180 min

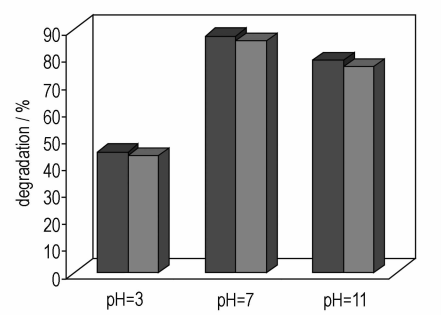

Fig. 8 Photodegradation of HMX (4.0 mg · L^{-1}, black color) and RDX (40.0 mg · L^{-1}, gray color) in acidic, neutral and basic solutions in the presence of CdS/Cu(5%) nanocatalyst with dosage 160.0 mg · L^{-1} after irradiation time of 180 min

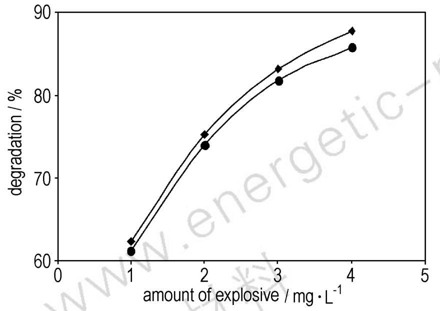

Fig. 9 Photodegradation of HMX (◆, $C_{HMX} \times 1$) and RDX (●, $C_{RDX} \times 10$) with different initial concentrations in neutral solutions in the presence of CdS/Cu(5%) nanocatalyst with dosage 160.0 mg · L^{-1} after irradiation time of 180 min

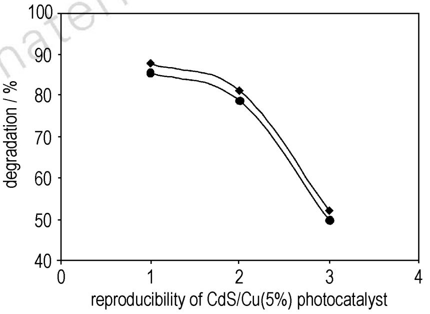

Fig. 10 Reproducibility of photoactivity of CdS/Cu(5%) nanocatalyst with dosage 160.0 mg · L^{-1} in photodegradation of HMX (◆, 4.0 mg · L^{-1}) and RDX (●, 40.0 mg · L^{-1}) after irradiation time of 180 min

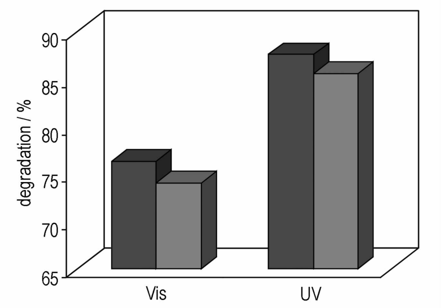

Fig. 11 Photodegradation of HMX (4.0 mg · L^{-1}, black color) and RDX (40.0 mg · L^{-1}, gray color) under UV and Vis irradiation in the presence of CdS/Cu(5%) nanocatalyst with dosage 160.0 mg · L^{-1} after irradiation time of 180 min

degradation of explosives under UV irradiation. The decrease of degradation yield is not unexpected because the energy of Vis light is less than UV.

4 Conclusions

The nitramine explosives such as HMX and RDX are destructed in the wastewaters by photodegradation under UV and/or Vis irradiation in the presence $Cd_{0.95}Cu_{0.05}S$ nanoparticles as photocatalyst. The degradation efficiency of both explosives reaches 85% -88% in the time duration of 180 min at pH 7 and at room temperature. The kinetics of the photodegradation in the presence of the nanocatalysts follows a first-order rate model. The reproducibility of proposed photocatalyst shows a decrease of activity after the first and second cycles.

References:

[1] Hu C, Wang Y Z. Decolorization and biodegradability of photocatalytic treated azo dyes and wool textile wastewater[J]. *Chemosphere*, 1999, 39: 2107 -2115.

[2] Kiwi J, Pulgarine C M, Gratzel P P. Beneficial effects of homogeneous photo-Fenton pretreatment upon the biodegradation of anthraquinone sulfonate in waste water treatment[J]. *Appl Catal B: Environ*, 1993, 3: 85 -99.

[3] Hoffman M R, Martin S T, Choi W, et al. Environmental applications of semiconductor photocatalysis[J]. *Chem Rev*, 1995, 95: 69 -96.

[4] Kansal S K, Singh M, Sud D. Studies on photodegradation of two commercial dyes in aqueous phase using different photocatalyst[J]. *J Hazard Mater*, 2007, 141: 581 -590.

[5] Liu Y, Chen X, Li J, et al. Photocatalytic degradation of azo dyes by nitrogen-doped TiO_2 nanocatalyst[J]. *Chemosphere*, 2005, 61: 11 -18.

[6] Aarthi T, Narahari P, Madras G. Photocatalytic degradation of Azure and Sudan dyes using nano TiO_2[J]. *J Hazardous Materials*, 2007, 149: 725 -734.

[7] Artemyev MV, Gurinovich L I, Stupak A P, et al. Luminescence of CdS nanoparticles doped with Mn[J]. *Phys Stat Sol*, 2001, 224: 191 -194.

[8] Dutta P, Fendler J H. Preparation of cadmium sulfide nanoparticles in self-reproducing reversed micelles[J]. *J Colloid Interface Sci*, 2002, 247: 47 -53.

[9] Tang H, Yan M, Zhang H, et al. Preparation and characterization of water-soluble CdS nanocrystals by surface modification of ethylene diamine[J]. *Materials Letters*, 2005, 59: 1024 -1027.

[10] Lu X, Mao H, Zhang W, et al. Synthesis and characterization of CdS nanoparticles in polystyrene microfibers[J]. *Materials Letters*, 2007, 61: 2288 -2291.

[11] Agostiano A, Catalano M, Curri M L, et al. Synthesis and structural characterisation of CdS nanoparticles prepared in a four-components " water-in-oil" microemulsion[J]. *Micron*, 2000, 31: 253 -258.

[12] Wang G Z, Chen W, Liang C H, et al. Preparation and characterization of CdS nanoparticles by ultrasonic irradiation[J]. *Inorganic Chem Commu*, 2001, 4: 208 -210.

[13] Heilmann H M, Weismann U, Stenstrom M K. Kinetics of the alkaline hydrolysis of high explosives RDX and HMX in aqueous solution and adsorbed to activated carbon[J]. *Environ Sci Technol*, 1996, 30: 1485 -1492.

[14] Liu Z, He Y, Li F, et al. Photocatalytic treatment of RDX wastewater with nano-sized titanium dioxide[J]. *Environ Sci Pollut Res Int*, 2006, 13: 328 -332.

[15] Hundal LS, Singh J, Bier E L, et al. Removal of TNT and RDX from water and soil using iron metal[J]. *Environ Pollut*, 1997, 97: 55 -64.

[16] Burton D T, Turley S D, Peters G T. The acute and chronic toxicity of hexahydro-1, 3, 5-trinitro-1, 3, 5-triazine (RDX) to the fathead minnow (Pimephales promelas)[J]. *Chemosphere*, 1994, 29: 567 -579.

[17] Burton D T, Turley S D, Peters G T. The toxicity of hexahydro-1, 3, 5-trinitro-1, 3, 5-triazine (RDX) to the freshwater green alga selenastrum-capricornutum[J]. *Water Air Soil Pollut*, 1994, 76: 449 -457.

[18] Peters G T, Burton D T, Paulson R L, et al. The acute and chronic toxicity of hexahydro-1, 3, 5-trinitro-1, 3, 5-triazine (RDX) to 3 freshwater invertebrates[J]. *Environ Toxicol Chem*, 1991, 10: 1073 -1081.

[19] McLellan W, Hartley W R, Brower M. Health advisory for hexahydro-1, 3, 5-tetranitro-1, 3, 5-triazine[R]. Technical Report No. PB90 -273533. Office of Drinking Water, US Environmental Protection Agency, Washington, DC, 1988.

[20] Etnier E L, Hartley W R. Comparison of water quality criterion and lifetime health advisory for hexahydro-1, 3, 5-trinitro-1, 3, 5-triazine (RDX)[J]. *Regulatory Toxicol Pharmacol*, 1990, 11: 118 -122.

[21] Spalding R F, Fulton J W. Groundwater munitions residues and nitrate near Grand Island, Nebraska, USA. Contam Hydrol 1988, 2, 139 -153.

[22] Pattabi M, Uchil J. Synthesis of cadmium sulfide nanoparticles[J]. *Solar Energy Materials and Solar Cells*, 2000, 63: 309 -314.

[23] Wang G Z, Chen W, Liang C H, et al. Preparation and characterization of CdS nanoparticles by ultrasonic irradiation[J]. *Inorganic Chemistry Communications*, 2001, 4: 208 -210.

[24] de Fariasa P M A, Santos B S, Longoc R L, et al. CdS nanoparticles: Structural and energetical correlations[J]. *Material Chemical Physics*, 2005, 89: 21 -28.

[25] Yang H, Huang C, Li X, et al. Luminescent and photocatalytic properties of cadmium sulfide nanoparticles synthesized via microwave irradiation[J]. *Materials Chemistry and Physics*, 2005, 90: 155 -158.

[26] Daneshvar N, Salari S, Khataee A R. Photocatalytic degradation of zao dye acid red 14 in water on ZnO as an alternative catalyst to TiO_2[J]. *J Photochem Photobiol A: Chem*, 2003, 157: 111 -116.

[27] Choi J K, Son H S, Kim T S, et al. Degradation kinetics and mechanism of RDX and HMX in TiO_2 photocatalysis[J]. *Environ Technol*, 2006, 27: 21 -232.

[28] Beydoun D, Amal R, Low G, et al. Role of nanoparticles in photocatalysis[J]. *J Nanoparticle Res*, 1999, 1: 439 -458.

[29] Barakat M A, Schaeffer H, Hayes G, et al. Photocatalytic degradation of 2-chlorophenol by co-doped TiO_2 nanoparticles[J]. *Appl Catal B: Environmental*, 2004, 57: 23 -30.

[30] Shah S I, Li W, Huang C P, et al. Study of Nd^{3+}, Pd^{2+}, Pt^{4+} and Fe^{3+} dopants effect on the photoreactivity of TiO_2 nanoparticles[J]. *Colloquium*, 2002, 99: 6482 – 6486.

[31] Yang X, Xu L, Yu X, et al. One-step preparation of silver and indium oxide co-doped TiO_2 photocatalyst for the degradation of rhodamine B [J]. *Catalysis Communications*, 2008, 9: 1224 – 1229.

[32] Kudo A, Niishiro R, Iwase A, et al. Effects of doping of metal cations on morphology, activity, and visible light response of photocatalysts [J]. *Chemical Physics*, 2007, 339: 104 – 110.

[33] Zhang F L, Zhao J C, Shen T, et al. TiO_2-assisted photodegradation of dye pollutants II. Adsorption and degradation kinetics of eosin in TiO_2 dispersions under visible light irradiation[J]. *Appl Catal B: Environmental*, 1998, 15: 147 – 156.

[34] Rashed M N, El-Amin A A. Photocatalytic degradation of methyl orange in aqueous TiO_2 under different solar irradiation sources[J]. *International J Physical Sci*, 2007, 2: 73 – 81.

[35] Zhu C, Wang L, Kong L, et al. Photocatalytic degradation of AZO dyes by supported TiO_2 + UV in aqueous solution[J]. *Chemosphere*, 2000, 41: 303 – 309.

[36] Wang C C, Lee C K, Lu M D, et al. Photocatalytic degradation of C. I. Basic Violet 10 using TiO_2 catalysts supported by Y zeolite: An investigation of the effects of operational parameters [J]. *Dyes and Pigments*, 2008, 76: 817 – 824.

[37] Al-Kahali M S, Al-Kata'a N. pH effect on the photocatalytic degradation of the chlorpyrifus from insecticide morisban4 by ZnO in aqueous medium[J]. *Ass Univ Bull Environ Res*, 2006, 9: 23 – 31.

[38] Sobana N, Swaminathan M. The effect of operational parameters on the photocatalytic degradation of acid red 18 by ZnO[J]. *Separation and Purification Techn*, 2007, 56: 101 – 107.